GHz-bandwidth upconversion detector using a unidirectional ring cavity to reduce multilongitudinal mode pump effects

Meng, Lichun; Høgstedt, Lasse; Tidemand-Lichtenberg, Peter; Pedersen, Christian; Rodrigo, Peter John

Published in:
Optics Express

Link to article, DOI:
10.1364/OE.25.014783

Publication date:
2017

Document Version
Publisher's PDF, also known as Version of record

Research Article | Vol. 25, No. 13 | 26 Jun 2017 | OPTICS EXPRESS 14783
Optics EXPRESS

GHz-bandwidth upconversion detector using a unidirectional ring cavity to reduce multilongitudinal mode pump effects

LICHUN MENG,[1,*] LASSE HØGSTEDT,[2] PETER TIDEMAND-LICHTENBERG,[1] CHRISTIAN PEDERSEN,[1] AND PETER JOHN RODRIGO[1]

[1]*DTU Fotonik, Department of Photonics Engineering, Technical University of Denmark, Frederiksborgvej 399, 4000 Roskilde, Denmark*
[2]*IRSee ApS, Frederiksborgvej 399, 4000 Roskilde, Denmark*
**licme@fotonik.dtu.dk*

Abstract: We demonstrate efficient upconversion of modulated infrared (IR) signals over a wide bandwidth (up to frequencies in excess of 1 GHz) via cavity-enhanced sum-frequency generation (SFG) in a periodically poled $LiNbO_3$. Intensity modulated IR signal is produced by combining beams from two 1547 nm narrow-linewidth lasers in a fiber coupler while tuning their wavelength difference down to 10 pm or less. The SFG crystal is placed inside an Nd:YVO_4 ring cavity that provides 1064 nm circulating pump powers of up to 150 W in unidirectional operation. Measured Fabry-Pérot spectrum at 1064 nm confirms the enhanced spectral stability from multiple to single longitudinal mode pumping condition. We describe analytically and demonstrate experimentally the deleterious effects of using a multimode pump to the high-bandwidth RF spectrum of the 630 nm SFG output. Offering enhanced sensitivity without the need for cooling, the GHz-bandwidth upconverter can readily be extended to the mid-IR (2 – 5 μm) as an alternative to cooled low-bandgap semiconductor detectors for applications such as high-speed free-space optical communications.

OCIS codes: (190.0190) Nonlinear optics; (190.7220) Upconversion; (040.0040) Detectors; (040.3060) Infrared.

References and links

1. A. Rogalski, "History of infrared detectors," Opto-Electron. Rev. **3**, 279–308 (2012).
2. Newport technical note, "Optical detection systems," https://www.newport.com/n/optical-detection-systems.
3. R. V. Roussev, C. Langrock, J. R. Kurz, and M. M. Fejer, "Periodically poled lithium niobate waveguide sum-frequency generator for efficient single-photon detection at communication wavelengths," Opt. Lett. **29**(13), 1518–1520 (2004).
4. C. Langrock, E. Diamanti, R. V. Roussev, Y. Yamamoto, M. M. Fejer, and H. Takesue, "Highly efficient single-photon detection at communication wavelengths by use of upconversion in reverse-proton-exchanged periodically poled $LiNbO_3$ waveguides," Opt. Lett. **30**(13), 1725–1727 (2005).
5. H. Pan and H. Zeng, "Efficient and stable single-photon counting at 1.55 μm by intracavity frequency upconversion," Opt. Lett. **31**(6), 793–795 (2006).
6. M. A. Albota and F. N. C. Wong, "Efficient single-photon counting at 1.55 μm by means of frequency upconversion," Opt. Lett. **29**(13), 1449–1451 (2004).
7. H. Pan, H. Dong, H. Zeng, and W. Lu, "Efficient single-photon counting at 1.55 mm by intracavity frequency upconversion in a unidirectional ring laser," Appl. Phys. Lett. **89**(19), 191108 (2006).
8. H. Pan, E. Wu, H. Dong, and H. Zeng, "Single-photon frequency up-conversion with multimode pumping," Phys. Rev. A **77**(3), 033815 (2008).
9. J. S. Pelc, G.-L. Shentu, Q. Zhang, M. M. Fejer, and J.-W. Pan, "Up-conversion of optical signals with multi-longitudinal-mode pump lasers," Phys. Rev. A **86**(3), 033827 (2012).
10. K.-D. F. Büchter, H. Herrmann, C. Langrock, M. M. Fejer, and W. Sohler, "All-optical Ti:PPLN wavelength conversion modules for free-space optical transmission links in the mid-infrared," Opt. Lett. **34**(4), 470–472 (2009).
11. R. Martini, C. Gmachl, J. Falciglia, F. G. Curti, C. G. Bethea, F. Capasso, E. A. Whittaker, R. Paiella, A. Tredicucci, A. L. Hutchinson, D. L. Sivco, and A. Y. Cho, "High-speed modulation and free-space optical audio/video transmission using quantum cascade lasers," Electron. Lett. **37**(3), 191–193 (2001).
12. R. Paiella, F. Capasso, C. Gmachl, C. G. Bethea, D. L. Sivco, J. N. Baillargeon, A. L. Hutchinson, A. Y. Cho, and H. C. Liu, "Generation and detection of high-speed pulses of mid-infrared radiation with intersubband semiconductor lasers and detectors," IEEE Photonics Technol. Lett. **12**(7), 780–782 (2000).

#296270 https://doi.org/10.1364/OE.25.014783
Journal © 2017 Received 18 May 2017; revised 13 Jun 2017; accepted 13 Jun 2017; published 19 Jun 2017

Optics EXPRESS

13. P. M. Henry, J. K. Powers, R. L. Rawe, and H. B. Morris, "HgCdTe photodiodes for heterodyne applications," Proc. SPIE **0663**, 145–154 (1986).
14. J. S. Dam, P. Tidemand-Lichtenberg, and C. Pedersen, "Room-temperature mid-infrared single-photon spectral imaging," Nat. Photonics **6**(11), 788–793 (2012).
15. J. Q. Zhao, Y. Z. Wang, B. Q. Yao, and Y. L. Ju, "High efficiency, single-frequency continuous wave Nd:YVO4/YVO4 ring laser," Laser Phys. Lett. **7**(2), 135–138 (2010).
16. M. Mancinelli, A. Trenti, S. Piccione, G. Fontana, J. S. Dam, P. Tidemand-Lichtenberg, C. Pedersen, and L. Pavesi, "Mid-infrared coincidence measurements on twin photons at room temperature," Nat. Commun. **8**, 15184 (2017).

1. Introduction

Frequency upconversion is a method for efficiently converting low-energy photons to high-energy photons by mixing the former with a high-field pump in a nonlinear crystal – thereafter, detecting at the shorter wavelength regime where more sensitive detectors exist. Over the years, the interest in using frequency upconversion to detect infrared (IR) signals has grown in many fields including spectroscopy, remote sensing, imaging, and communications. For IR detection, frequency upconversion is an attractive technology because the specific detectivity D* of conventional IR detectors (most notably, low-bandgap semiconductors like HgCdTe and microbolometers) are several orders of magnitude lower than that of Si based photodetectors [1, 2]. Furthermore, Si detectors/cameras operate at room-temperature while HgCdTe detectors require stringent cooling to achieve sufficient suppression of dark noise.

Broadly speaking, IR upconverters can be classified as either single-pass pumped or cavity-enhanced. In single-pass type upconverters, both the IR signal and the pump transmit through the nonlinear crystal only once. High intensity single-pass (nonresonant) pumping – therefore, high conversion efficiency – is usually achieved by using a waveguide nonlinear crystal [3] wherein the upconversion or sum-frequency generation (SFG) process can be strongly confined in a single spatial mode. A maximum internal conversion efficiency exceeding 90% and an overall detection efficiency of 46% have been achieved in a single-pass upconverter for 1.56 μm signal using a 50-mm long periodically poled lithium niobate (PPLN) waveguide and a 1064 nm pump with power in the order of 100 mW [4]. On the other hand, upconverters with cavity enhancement achieve high pump intensities by incorporating a bulk nonlinear crystal inside a resonant cavity, for example, inside an Nd:YVO_4 laser resonator (i.e. intracavity upconverters) [5]. In this way, high circulating pump powers of several tens (or hundreds of Watts depending on pump beam waist size) allow for the upconversion of the single-pass IR signal with the maximum possible conversion efficiency. Pan and Zeng [5] have achieved an internal conversion efficiency of 74% with 80.5 W of circulating pump. An internal conversion efficiency of 90% (overall efficiency of 59%) has also been achieved for another upconverter in which the 1064 nm pump laser is external to the resonant cavity, at a circulating power of 23 W [6].

Intracavity upconverters relying on a linear Nd:YVO_4 cavity have been observed to operate in multilongitudinal pump modes [5]. It has been previously proposed that, instead of a standing-wave cavity, the use of a ring cavity with a non-reciprocal element (e.g. an optical isolator) can force the 1064 nm pump to propagate unidirectionally [7, 8]. This results in a more spectrally stable pump since the spatial hole burning in the Nd:YVO_4 crystal is significantly suppressed. A higher maximum conversion efficiency and a lower standard deviation of the SFG output intensity was experimentally observed for the ring cavity system than for the standing-wave cavity [7]. However, no sufficient data were presented in these previous studies to establish that the circulating pump operated in a single longitudinal mode even with a ring cavity. In [8], Pan *et al.* were unable to observe any significant effect to the SFG output even if the ring cavity 1064 nm pump was made to run in an increased number of longitudinal modes. This is likely due to their detector sampling rate being too low compared to the pump beat frequencies. Pan and co-authors [8] also proposed a model to describe the interaction between a quantum signal and the multimode pump but it failed to account for temporal fluctuations of the instantaneous pump intensity due to the beating of the oscillating

Optics EXPRESS

modes. This model was later amended in the work of Pelc *et al.* [9] which demonstrated that a penalty of using a multimode pump (versus single mode) is the reduction of the maximum achievable average conversion efficiency. Pelc and co-authors used an unmodulated (or DC) IR signal and only measured the RF spectrum of the unconverted part of this IR signal, which was found to inherit the beat frequencies associated with the pump.

Here we extend the investigation to study the properties of a high-bandwidth intracavity upconversion detector that uses a bulk PPLN inside a 1064 nm Nd:YVO_4 unidirectional ring cavity – comparing single mode versus multilongitudinal mode operation. The upconverter is described by a transfer function, which characterizes the capacity of the detector to transfer the fast modulation of the input IR signal, at a given frequency, to the SFG output. In this study, the transfer function is examined over a wide range of frequencies (up to GHz level) using FFT spectral analysis. This allows us to characterize the performance of the upconverter for high-speed, i.e. high-bandwidth, detection applications. Simultaneous FFT analyses of the GHz-sampled instantaneous powers of the input IR signal, the SFG output, as well as the small 1064 nm pump leakage through a cavity mirror allow us to quantitatively demonstrate the upconverter's performance and how it is influenced by the pump operating in multilongitudinal mode versus single mode. Furthermore, the optical spectrum of the 1064 nm pump that leaks out of another cavity mirror is also monitored using a high-finesse scanning Fabry-Pérot interferometer (FPI) to directly track the number of longitudinal modes. The improved single longitudinal mode pump operation achieved with a unidirectional ring cavity design enables the upconverter to be useful over a wide range of frequencies free from undesirable effects of the 1064 nm mode beating. In other words, the SFG output has a Fourier spectrum that closely mimics that of the original IR signal. Some applications of the GHz-bandwidth upconversion detector, when extended to 2 – 5 μm, are free-space optical communications [10, 11], pulse laser temporal profiling (e.g. accurate rise-time and fall-time measurements) [12] or modulation frequency response characterization [11] of mid-IR quantum-cascade lasers and optical parametric oscillators, and IR heterodyne detection [13].

2. Theory

The conversion efficiency η is normally considered as a constant in upconversion detection if the average pump power is stable. Obviously, this is a good assumption for the weak and low-bandwidth signal detection. But in the general case (especially at sufficiently short temporal scales), η may fluctuate over time due to variations in the instantaneous pump power $P_p(t)$, for example, when the pump is lasing with multilongitudinal modes. If the frequency components of the pump fluctuation are comparable to the signal frequency, it will induce extra noise for the detection and thereby degrade the signal-to-noise ratio (SNR). Before applying the upconversion detector for high-bandwidth IR signal detection, we first develop a model to calculate the transfer function of the upconverter and investigate the effects of multimode pumping on the spectrum of the SFG output.

2.1 Derivation of the transfer function of the high-bandwidth upconverter

In our physical model, an IR input field $a_{IR}(t)$ with frequency ν_{IR} interacts with a strong pump field $a_p(t)$ with frequency ν_p in a periodically poled nonlinear crystal of length L. The upconversion process results in an SFG output field $a_{up}(t)$ with frequency $\nu_{up} = \nu_{IR} + \nu_p$. We consider the case of plane-wave interaction and non-depletion of the optical pump. Moreover, the interaction time of the three fields in the crystal is assumed to be much shorter than the time scales associated with (i) the pump power fluctuation [9], and (ii) the IR signal (and SFG output) modulation. The coupled equations for a_{IR} and a_{up} are given by:

Optics EXPRESS

$$\frac{\partial a_{IR}(z,t)}{\partial z} = -i\kappa a_p^*(t) a_{up}(z,t)\exp(-i\Delta k z), \tag{1}$$

$$\frac{\partial a_{up}(z,t)}{\partial z} = -i\kappa a_p(t) a_{IR}(z,t)\exp(i\Delta k z). \tag{2}$$

The phase mismatch of the SFG process is given by $\Delta k = \left|k_{IR} + k_p + k_{up}\right| - 2\pi/\Lambda$, where Λ is the PPLN poling period. For each wavelength, k_j is the wavevector magnitude in the PPLN and a_j is a normalized field such that $\left|a_j\right|^2$ gives the photon rate. The coupling coefficient κ:

$$\kappa = 2\pi\varepsilon_0 d_{eff}\Theta\left[2h\nu_{IR}\nu_p\nu_{up}Z_0^{\,3}/(n_{IR}n_p n_{up})\right]^{1/2}, \tag{3}$$

where d_{eff} is the PPLN's effective nonlinear coefficient, n_j is its refractive index, Θ is the mode-overlap integral, h is the Planck constant, ε_0 and $Z_0 = \sqrt{\mu_0/\varepsilon_0}$ are the vacuum permittivity and impedance, respectively (where μ_0 is the vacuum permeability).

If the quasi-phase-matching condition is fulfilled with $\Delta k = 0$, the solutions to Eqs. (1) and (2) take the following form:

$$a_{IR}(L,t) = a_{IR}(0,t)\cos\left[\kappa\left|a_p(t)\right|L\right] + a_{up}(0,t)\sin\left[\kappa\left|a_p(t)\right|L\right], \tag{4}$$

$$a_{up}(L,t) = -a_{IR}(0,t)\sin\left[\kappa\left|a_p(t)\right|L\right] + a_{up}(0,t)\cos\left[\kappa\left|a_p(t)\right|L\right]. \tag{5}$$

For the case of IR signal detection, in which $a_{up}(0,t) = 0$, the field amplitude of the upconversion (SFG output) signal can be simplified as:

$$a_{up}(L,t) = -a_{IR}(0,t)\sin\left[\kappa\left|a_p(t)\right|L\right]. \tag{6}$$

The time-dependent conversion efficiency can then be written as:

$$\eta(t) = \left|a_{up}(L,t)\right|^2 / \left|a_{IR}(0,t)\right|^2 = \sin^2\left[\kappa\left|a_p(t)\right|L\right]. \tag{7}$$

Let the normalized frequency spectra of the photon rates $\left|a_{IR}(0,t)\right|^2$ and $\left|a_{up}(L,t)\right|^2$ be:

$$\tilde{N}_{IR}(f) = b_1 \boldsymbol{F}\left\{\left|a_{IR}(0,t)\right|^2\right\}, \tag{8}$$

$$\tilde{N}_{up}(f) = b_2 \boldsymbol{F}\left\{\left|a_{up}(L,t)\right|^2\right\}, \tag{9}$$

where $\boldsymbol{F}$ denotes the Fourier transform operator operating on variable t, and b_1 and b_2 are constants upon normalization of the spectra by their respective zero-frequency components. In this study, we describe the detector system by a normalized transfer function $\tilde{H}(f)$ such that:

$$\tilde{N}_{up}(f) = \tilde{H}(f)\tilde{N}_{IR}(f). \tag{10}$$

Combining Eqs. (7)-(10), we get the modulus of the transfer function:

Optics EXPRESS

$$\left|\tilde{H}(f)\right| = \frac{b\left|\mathcal{F}\left\{\left|a_{IR}(0,t)\right|^2\right\} \otimes \mathcal{F}\{\eta(t)\}\right|}{\left|\mathcal{F}\left\{\left|a_{IR}(0,t)\right|^2\right\}\right|}, \tag{11}$$

where $\otimes$ is the temporal convolution operator and b is a constant such that $\left|\tilde{H}(f)\right| = 1$.

When the upconverter is pumped with a single longitudinal mode laser, $a_p(t)$ is essentially constant, and so is $\eta(t)$, for temporal scales greater than or equal to the inverse of the detector bandwidth. If η is independent of time, then $\left|\tilde{H}(f)\right|$ is unity within the detector bandwidth. However, when the pump operates in multilongitudinal mode, its instantaneous power $P_p(t)$ will fluctuate leading to a more complicated frequency response of the upconverter.

2.2 The case of two longitudinal pump modes

For the case of two-mode pumping, the instantaneous pump power is no longer constant:

$$P_p(t) = P_{ave}\left[1 + \alpha\cos(2\pi\Delta f t + \varphi)\right], \tag{12}$$

where $P_{ave} = h\nu_p\left\langle\left|a_p(t)\right|^2\right\rangle$ is the average pump power, α is the contrast of the sinusoidal power variation due to mode-beating, Δf is the mode frequency spacing, and φ is an arbitrary phase. From Eqs. (7) and (12), $\eta(t)$ can be expressed (for the two-mode case) as:

$$\eta(t) = \sin^2\left[\frac{\pi}{2}\sqrt{\left(\frac{P_{ave}}{P_{max}}\right)\left|1 + \alpha\cos(2\pi\Delta f t + \varphi)\right|}\right], \tag{13}$$

where $P_{max} = \pi^2 h\nu_p / (4\kappa^2 L^2)$. Examples of instantaneous pump power fluctuations are shown in Fig. 1(a). The corresponding conversion efficiency $\eta(t)$ and the magnitude of its spectrum $\mathcal{F}\{\eta(t)\}$ are shown in Figs. 1(b) and 1(c), respectively. Figure 1(c) reveals that the spectrum of η for the dual mode case may have several frequency components at $f = m\Delta f$ ($m = 0, 1, 2, \ldots$) and not only limited to components at $f = 0$ and $f = \Delta f$.

The red curve in Fig. 1 shows the case of $P_{ave} = P_{max}$ and unity contrast. It is characterized by the presence of strong higher order peaks in its conversion efficiency Fourier spectrum. The green curve is also for $\alpha = 1$ but with a lower $P_{ave} = 0.25P_{max}$. The blue curve is for $\alpha = 0.05$ and $P_{ave} = 0.25P_{max}$, which corresponds to $\eta_{ave} = 50\%$ or close to the operating point in our experiment. We observe that the non-zero frequency components become weaker with decreasing α (with $\alpha = 0$ resulting in the single mode case). The black curve simulates the case of $\alpha = 0.5$ and a relatively low average conversion efficiency obtained at $P_{ave} = 0.09P_{max}$, i.e. $\eta_{ave} = 20\%$, like those obtained with the upconversion system described in a previous work [14]. It shows that the component at $f = 2\Delta f$ is 17 dB lower than the component at $f = \Delta f$. This implies that higher order effects or frequency components larger than Δf are also reduced when operating at relatively low average conversion efficiency.

Optics EXPRESS

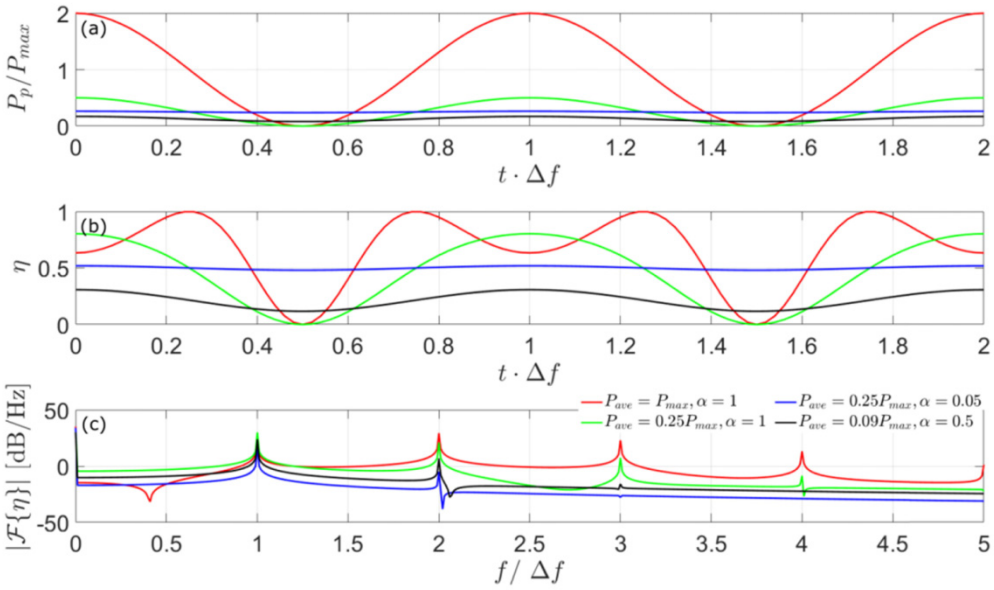

Fig. 1. (a) Instantaneous pump power P_p (normalized by P_{max}) versus time (normalized by the inverse of the mode frequency spacing Δf) for four different combinations of average pump power and contrast that describe the beating of two pump axial modes, (b) corresponding instantaneous conversion efficiency given by Eq. (13), and (c) magnitude of the FFT of conversion efficiency curves shown in (b).

3. Experimental setup

In order to achieve high-bandwidth IR signal detection with frequency upconversion, we chose a unidirectional ring cavity configuration for high-power pumping of our upconverter. In comparison to the linear (or standing-wave) cavity, the unidirectional ring cavity design is more capable of stable lasing at a single longitudinal mode due to the inhibition of spatial hole burning [7, 15]. The schematic diagram of the upconverter is shown in Fig. 2(a).

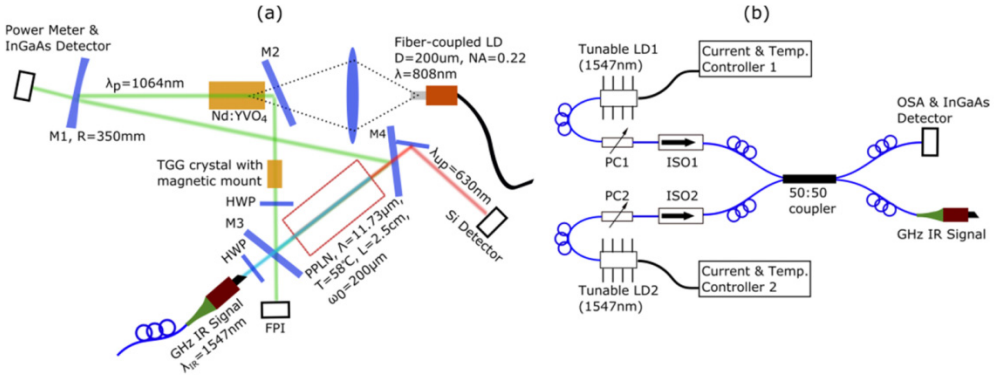

Fig. 2. (a) High-bandwidth IR upconversion detector based on a unidirectional ring cavity and (b) intensity modulated signal generator with a central wavelength of 1547 nm and modulation frequency tuning up to GHz.

The laser crystal Nd:YVO_4 (*a*-cut, 3 mm × 3 mm × 8 mm, 0.5% Nd-doped) is pumped by a fiber-coupled laser diode (Laser Components 808nm-mm-hhl-fiber-10w, λ = 808 nm, fiber core diameter = 200 μm, *NA* = 0.22, and maximum optical power = 10 W). The laser cavity consists of four mirrors (M1, M2, M3 and M4) with high reflectance (>99.9%) at 1064 nm for s-polarization state. M1 is a concave mirror with radius of curvature R = 350 mm, while M2,

Optics EXPRESS

M3 and M4 are plane mirrors. M3 is the IR signal coupling mirror with a transmittance >90% at 1547 nm and M4 is the SFG output signal decoupler with a transmittance >82% at 630 nm. Due to an optical isolator: a terbium gallium garnet (TGG) crystal mounted in a ferromagnetic ring followed by a half wave plate (HWP), and the mirrors' higher reflectance for s-polarization than for p-polarization at oblique incidence, the 1064 nm pump propagates unidirectionally. A 25-mm long bulk PPLN is placed between M3 and M4. The 1064 nm beam waist radius ω_0 in the PPLN crystal is ~200 μm. The PPLN has a poling period Λ = 11.73 μm and its temperature is kept at T = 58 °C to maximize the conversion efficiency.

Figure 2(b) shows the schematic diagram of the modulated IR signal generator. Two identical fiber-coupled narrow-linewidth laser diodes (LD1 and LD2) with central wavelength around 1547 nm are combined through a polarization-maintaining fiber splitter/combiner (50:50 split ratio). One fiber coupler output is used to monitor the IR signal directly with a fast detector and/or connected to an optical spectrum analyzer (OSA) for coarse-tuning of the wavelength difference. The other output serves as the IR signal of the upconverter in Fig. 2(a). The modulation frequency f_M (proportional to the wavelength difference of LD1 and LD2) can be varied from near-zero to ~1 GHz, with a stability of a few MHz, by tuning either the temperature or the drive current of the two laser diodes. We also maximized the interferometric contrast by balancing the output power of the two lasers. To minimize both insertion loss and optical feedback, polarization controllers (PC1 and PC2) and fiber isolators (ISO1 and ISO2) are attached to the laser diodes. This setup is also able to create challenging modulation frequencies extending to 10 – 100 GHz, relevant for high-speed communications.

4. Experimental results

During our experiments, the 808 nm laser diode is set at an output of 6.5 W, which can maintain a 1064 nm intracavity circulating pump power of 147 W. The average power of the 1547 nm signal used is 2.1 mW and the resulting average power of the 630 nm SFG signal coming out of the upconverter is 2.17 mW. Considering 80% total transmission at 630 nm through M4 and a bandpass filter, the average internal conversion efficiency $\eta_{ave} = 52.7\%$. We have optimized the cavity alignment to achieve a single transverse mode profile for the 1064 nm pump at a relatively high 147 W pump power operating point. At some other pump power values, the 1064 nm pump tends to operate at multiple transverse modes – making it difficult to reliably measure the dependence of the conversion efficiency on pump power.

The number of longitudinal modes of the 1064 nm pump is monitored with a scanning Fabry-Pérot interferometer (FPI). The FPI spectra are shown in Fig. 3 for the case of multiple and single longitudinal mode lasing. The upconverter can be optimized for single frequency pump operation by aligning the cavity mirrors and the rotational position of the HWP.

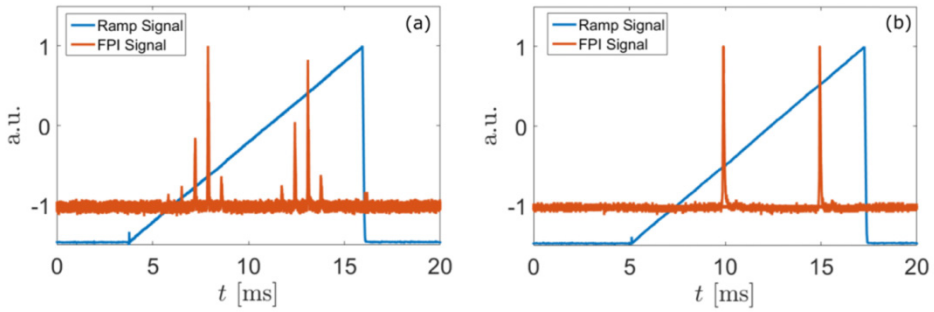

Fig. 3. Scanning FPI spectrum of the 1064 nm pump in (a) multiple and (b) single longitudinal mode operation. The spectra are stable for durations longer than our typical measurement time.

Optics EXPRESS

To evaluate the performance of the upconverter, the 1547 nm signal and the 1064 nm pump are measured with two InGaAs detectors (Thorlabs DET08CFC/M and DET08CL/M), the 630 nm SFG signal is measured with a Si detector (Thorlabs DET025AFC/M). All three detectors have bandwidths exceeding 2 GHz. Output voltages of the detectors are simultaneously monitored by an oscilloscope (LeCroy 104MXs-B, 3-dB bandwidth = 1 GHz).

The Fourier spectra of the photon rates (or power) of all three interacting waves are obtained by taking the FFT of their respective detector signals which are sampled by the oscilloscope at 5 GS/s for 5 μs. Figures 4(a) to 4(f) compare the magnitude of all normalized spectra when the pump operates in multimode and single longitudinal mode. Figure 4(c) shows that when the 1064 nm pump runs in multilongitudinal mode (for example, when M3 is slightly misaligned and/or the HWP is at a suboptimal position that degrades optical isolation), it exhibits several beat frequencies at $f = m\Delta f$ (for $m = 1, 2, 3, \ldots$), where Δf = 603.6 MHz. The free spectral range (FSR) of the ring cavity is given by:

$$\mathrm{FSR} = c \Big/ \sum_i n_i l_i \,, \tag{14}$$

where n_i and l_i are the refractive index and the length of the i-th medium along the path of the pump in a round-trip. According to Eq. (14), the calculated FSR of our cavity is 616 ± 25 MHz, which is in good agreement with the observed Δf from the 1064 nm Fourier spectrum. It validates that the multilongitudinal mode lasing is the main reason for the fluctuation of the 1064 nm pump power shown in Fig. 4(c).

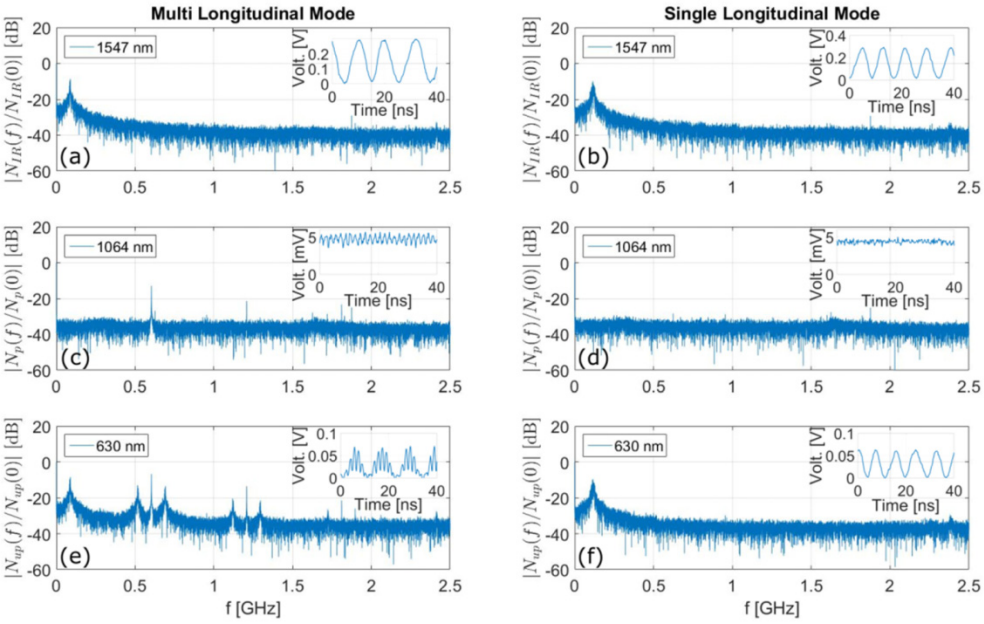

Fig. 4. Modulus of the FFT spectra of simultaneously detected powers of (a), (b) the 1547 nm signal, (c), (d) the 1064 nm pump, and (e), (f) the 630 nm SFG output for (a), (c), (e) multimode and (b), (d), (f) single longitudinal mode pump operation. Each inset shows a time series of the detected instantaneous power (i.e. InGaAs or Si detector voltage) for the respective wavelength. Each FFT spectrum is normalized by their zero-frequency component.

By analyzing Fig. 4(e) in detail, we discover that the peaks in the 630 nm spectrum can be separated into different groups based on their frequency spacing. We name these groups for the convenience of further discussion as follows: the fundamental group has only one peak at frequency $f = f_M$ = 88.4 MHz which corresponds to the original signal shown in Fig. 4(a);

Optics EXPRESS

the secondary group contains three peaks with $f = \Delta f$ and $f = \Delta f \pm f_M$; the tertiary group also contains three peaks with $f = 2\Delta f$ and $f = 2\Delta f \pm f_M$. Even higher order peak groups well beyond the 1 GHz bandwidth of the oscilloscope are observed but highly attenuated and thus ignored in the analysis. In contrast, Fig. 4(f) shows no additional spurious peaks for the spectrum of the SFG signal, i.e. only the original signal at $f = f_M =$ 116.2 MHz shown in Fig. 4(b) is reproduced, when the pump runs in single mode.

As we have presented in section 2, the 630 nm SFG Fourier spectrum can be calculated from the convolution of the FFT of the 1547 nm signal with the FFT of the conversion efficiency, which is revealed by Eq. (11). Alternatively, the appearance of the additional peaks in Fig. 4(e) can be explained in the following manner: it is perhaps obvious that the frequency sum $\Delta f + f_M$ and difference $\Delta f - f_M$ give rise to the side peaks of the secondary peak group. But the reason for the tertiary group is more complex. Figure 3(a) clearly shows that the 1064 nm pump has more than two oscillating modes. The beating of the two closest side-modes, one to the left and the other to the right of the strongest mode, gives rise to the frequency component at $f = 2\Delta f$, which is also confirmed by Fig. 4(c). Similarly, the frequency sum $2\Delta f + f_M$ and difference $2\Delta f - f_M$ contribute to the tertiary peak group. Additionally, the higher order frequency response of the detector ($\Delta f \rightarrow 2\Delta f$), see for example Fig. 1(c), may also contribute to the tertiary group. In other words, it is possible to observe the tertiary group even if there are only two longitudinal pump modes with mode spacing Δf.

The blue curve in Fig. 1(c) uses the parameters $\alpha = 0.05$ and $P_{ave} = 0.25P_{max}$, which are similar to those in our experimental result for the case of multimode pump operation (the amplitude of the peak at $f = \Delta f$ in Fig. 4(c) is –12.91 dB). This curve simulates the effect of higher order frequency response due to the beating of only two adjacent longitudinal modes. The simulation shows that the amplitude ratio between the peaks at $f = \Delta f$ and $f = 2\Delta f$ is 21 dB, which is quite larger than the measured amplitude ratio of 7 dB between the corresponding secondary and tertiary peaks shown in Fig. 4(e). The measured ratio would be even smaller had the oscilloscope bandwidth been large enough to accommodate the tertiary group. Therefore, we can draw the conclusion that the tertiary group of peaks is predominantly due to the beating of non-adjacent pump modes (separated by $2\Delta f$) instead of the higher order ($\Delta f \rightarrow 2\Delta f$) frequency response due to the adjacent pump mode beating.

In the following experiment, the transfer function of the upconversion detector with single mode pump is studied by tuning the modulation frequency f_M. During the measurement, the 1064 nm pump power remains constant and so does the conversion efficiency. The normalized FFT spectra of the 1547 nm signal and the 630 nm SFG output signal power are monitored simultaneously. Figures 5(a)-5(c) show the modulus of the two spectra for different f_M values. Figure 5(d) is the measured modulus of the normalized transfer function $\left|\tilde{H}(f)\right|$ of the upconversion detector which is relatively flat in the range ~0 to 1 GHz.

The theoretical model of our single axial mode pumped upconverter implies that the IR detector has the ability of measuring the signal with an unlimited bandwidth (or more precisely, limited only by the fast Si based detector that detects the SFG output). Figure 5(d) empirically proves that the modulus of the normalized transfer function is flat with less than ± 0.5 dB deviation from unity within DC to ~1 GHz. No further measurement is done due to the bandwidth limitation of our oscilloscope. If an electronic spectrum analyzer with several GHz of bandwidth is used, the effective detection bandwidth of the upconverter can instead become limited by the bandwidth of the Si detector for the SFG signal. In our experiments,

Optics EXPRESS

the oscilloscope limits our ability to accurately assess the transfer function of our upconverter above 1 GHz.

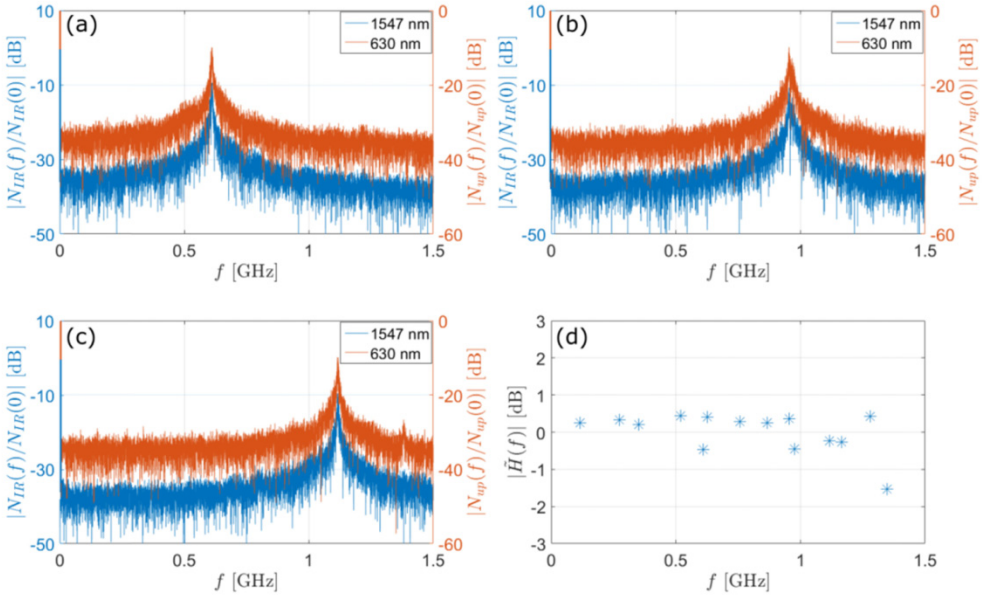

Fig. 5. Magnitude of the normalized FFT spectra of the 1547 nm input signal and the 630 nm SFG output power for single frequency pump operation and for signal modulation frequency of (a) 611.8 MHz, (b) 954.4 MHz, and (c) 1.19 GHz, and (d) the measured normalized transfer function of our GHz-bandwidth upconversion detector.

5. Discussion

To achieve optimal conversion efficiency with an upconversion detector, high-power pump lasers are usually employed. Since high-power pump sources tend to operate in multilongitudinal mode, Pan *et al.* [8] previously investigated theoretically and experimentally whether or not the quantum feature of incident signal photons is altered in the corresponding SFG photons when a multimode pumped upconverter is used. Theoretically, they assumed that the total pump intensity is given by the incoherent sum of the individual mode intensities. This model failed to capture the temporal fluctuations of the pump intensity caused by the beating of the modes, which was shown in a later work by Pelc *et al.* [9] to be correctly described by a coherent sum (i.e. summing the fields of the modes first before taking the squared modulus). The first study into the effects of multimode pumping in an upconverter initiated by Pan *et al.* also provided experimental results illustrating the intensity stability of the SFG output at high power levels of the pump in multimode operation. The implications of the beating of the pump modes were not revealed by their SFG intensity time-series (neither by its spectrum had it been shown). We think this is due to the fact that their SFG output was detected by a Si single-photon counting module, which typically has a limited photon count rate of about 10 MHz (i.e. single-photon counting upconverter bandwidth is well below the expected pump beat frequencies).

One can consider the results presented in our work as an extension of the study done by Pelc *et al.* [9]. However, our investigations differ from theirs in a number of aspects. We have expanded their model as well as their experiments to accommodate for amplitude modulated IR signals at modulation frequencies covering GHz-wide dynamic range. In the previous work, only a constant (or DC) IR signal was considered. Furthermore, we have simultaneously monitored the instantaneous power of our 1547 nm signal, the 1064 nm pump, and the 630 nm SFG output (and for different 1547 nm signal modulation frequencies in

Optics EXPRESS

either single or multilongitudinal pump mode operation). Pelc *et al.* only monitored their residual (1.55 μm) IR signal power, which they analyzed in terms of its RF spectrum. Using a DC 1.55 μm signal, they only showed experimentally that the mode beating of the pump is manifested in the spectrum of the residual IR signal. In our work, we have simultaneously measured the RF spectra of all three interacting waves, as shown in Fig. 4, demonstrating explicitly that the SFG output inherits the spectral peaks of the pump (caused by the beating of its modes) convolved with the spectrum of the IR signal. We have also performed a further confirmation of the single or multimode operation of the 1064 nm pump by sending it through a scanning FPI for high-resolution spectral analysis that allows us to determine the actual number of longitudinal modes present. In the previous work, no direct measurement of the number of pump modes was performed. Instead, the authors estimated the number of modes from the ratio of their pump laser spectral linewidth (measured by an OSA) and the FSR of the laser resonator. In our present study (due to the ability to achieve single longitudinal pump mode operation), we measured and confirmed that the upconverter has a uniform frequency response in a bandwidth as high as 1 GHz, as shown in Fig. 5 – in agreement with our model. In Pelc *et al.*, the upconverter was a single-pass type which used a PPLN waveguide and a fiber laser emitting a 1.94 μm pump with about 300 oscillating modes.

The theoretical model presented in section 2 provides a good description of the performance of our unidirectional ring cavity based upconverter operating in either single frequency or multilongitudinal mode operation. We however emphasize that the model, particularly for the multimode case, can be applied to other types of upconversion detectors like those based on linear cavity [5] or single-pass systems [9] as long as the instantaneous pump power fluctuation and its influence on the upconversion efficiency are accounted for.

Fluctuations of the pump power in a linear cavity can be neglected if its beat frequency is larger than the bandwidth of the RF signal. Theoretically, the beat frequency Δf is set by the cavity length. However, the maximum Δf is limited by the shortest cavity length we can implement in practice. For example, if the bandwidth of the RF signal is 10 GHz, the cavity length should not exceed 15 mm, which is unrealistic for linear intracavity upconverters. Furthermore, maximum average conversion efficiency near unity is only possible when single longitudinal mode pumping is used [9]. The ring cavity upconverter that has the potential for stable single frequency pump operation is therefore a better choice for high-bandwidth IR signal detection.

6. Summary and outlook

The implementation of an intracavity upconversion detection of sinusoidally modulated IR signals at 1547 nm with modulation frequencies as high as 1 GHz was presented in this work. A unidirectional Nd:YVO_4 ring cavity was employed to produce 1064 nm circulating pump powers reaching 150 W. Using a theoretical model, we showed that the upconverter's ability to transfer the sinusoidal intensity variation from the IR signal to the SFG output at 630 nm, with equally high fidelity at any modulation frequency is made possible by operating the pump in single longitudinal mode. Theoretical/numerical predictions also showed that for multimode pump operation, spurious noise spikes in the RF spectrum of the SFG output will appear due to a convolution of the spectral features of the conversion efficiency (due to the beating pump) with that of the IR signal. These noise peaks in the SFG output spectrum ultimately degrades the upconversion detector's SNR particularly for signal frequencies located near the noise peaks. Furthermore, multimode pump operation results in unwanted higher order replicas of the signal, which create ambiguities and thereby limit the effective bandwidth of the upconverter. Experimentally, we were able to demonstrate that the GHz-bandwidth upconverter running in single frequency pump operation has a uniform frequency response over a wide range of modulation frequencies (~0 to 1 GHz). The average internal conversion efficiency achieved by the presented upconverter was 52.7% (or an overall

Optics EXPRESS

detection efficiency of about 40%) at pump power of 147 W. Like Si based detectors, fast InGaAs detectors with bandwidths of several GHz are available and can be used for telecom wavelengths. However, our proposed GHz-upconverter can easily be extended to the mid-IR region (2 – 5 μm) by implementing minor changes to the PPLN period (i.e. change to $\Lambda > 20$ μm) and the surface coatings of the ring cavity optical components [14, 16]. Such mid-IR GHz-upconverter may serve as a better alternative to liquid-N_2 cooled HgCdTe photodetectors, not only for the elimination of cumbersome cooling requirements but also for significant enhancements in SNR. This variant of our high-bandwidth upconverter may find great potential in mid-IR related applications in wireless optical communications, heterodyne detection, and laser characterization [10–13].

Funding

Mid-TECH – H2020-MSCA-ITN-2014 (642661).